

Available online at [www.sciencedirect.com](http://www.sciencedirect.com)**ScienceDirect**

Energy Procedia 57 (2014) 2733–2742

Energy

**Procedia**

# Electrolytic nickel impregnation of porous anodic aluminum oxide films using AC voltage as solar selective absorber

Samuel Santiago and A.M. Fernandez \*

Instituto de Energías Renovables, Av. Xochicalco s/n Col Rubén Jaramillo, C.P. 62580, Temixco Morelos, México

---

## Abstract

Anodized aluminum oxide films on aluminum substrates 1050 (99.5% Al) was impregnated with nickel by electrodeposition technique. In these paper, we report the synthesis of Ni using the galvanostat mode, and also some experimental modification in the frequency and voltage values, in order to optimize the amount content of Ni on aluminum substrate. The data values of the total reflectance were analyzed in the visible solar spectrum and near infrared as a function of voltage, frequency and time of the impregnation process. Several experiments were performed in order to correlate these parameters with the nickel content in the bottom of the pores of the film and its reflectance properties. By morphological analysis found that samples with average nickel content of 10% of the total pore volume not exhibit good properties of a selective absorber, however the samples containing 60% of the total pore volume, present in the reflectance spectrum visible solar 5% and 90% in the infrared solar spectrum so it can be considered a good selective absorber films makes these coatings are prospects for implementation in solar collectors.

© 2014 The Authors. Published by Elsevier Ltd. This is an open access article under the CC BY-NC-ND license (<http://creativecommons.org/licenses/by-nc-nd/3.0/>).

Selection and/or peer-review under responsibility of ISES.

Key words: anodizing aluminum, porous anodic films of aluminum oxide, impregnation of nickel, Alternate current (AC), total reflectance

---

\* Corresponding author. Tel.: +52-55-56229705; fax: +52-55-56229742

E-mail address: [afm@ier.unam.mx](mailto:afm@ier.unam.mx).

## 1. Introduction

An alternative to harness solar energy is to convert part of the electromagnetic radiation to thermal energy (photothermal conversion). To accomplish this goal requires developing coatings and known as spectrally selective surfaces.

The possibility of practical development of selective absorbing surfaces was first demonstrated of Tabor (1955, 1961) and Gier and Dunkle(1955) [1-3] and others [4-5] who defined the basic concept of using spectral selectivity for efficient photothermal conversion of solar radiation. The concept was, and remains today, very simple produce a material that has a high absorbance  $\alpha$  ( $> 90\%$ ) in the range of solar radiation (mainly in the visible) low emittance  $\varepsilon(T)$  ( $<20\%$ ) in the range of thermal radiation (IR radiation). Spectral selective absorbing surfaces can be obtained by developing composite metal-dielectric coatings which are also referred to as cermet films. The reflectance spectrum of an ideal selective absorbing surface is shown in Figure 1.

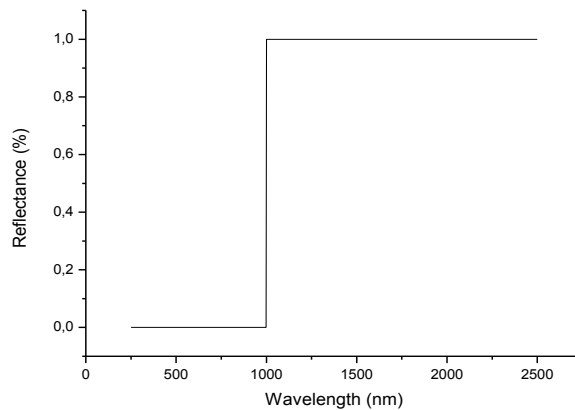


Figure 1. The reflectance spectrum of an ideal selective absorbing surface

From the Figure 1 it is possible to note that the reflectance increase the values in a point call wavelength  $\lambda_c$  that correspond to near infrared. Selective absorbing surfaces can be developed by chemical methods [6], physical [7] and electrochemical [8] used on steel substrates, zinc, copper and aluminium anodized. Aluminium anodized is frequently used as an encapsulating matrix of metal particles for producing absorbers materials solar radiation [9-10].

The process of developing a selective absorbing surface using electrochemical methods is performed in two stages, in the first step, the aluminium substrates are oxidized anodically where a porous film is created using Direct Current Voltage (DC) and in the second step, metallic nickel particles precipitated at the bottom of the pores, which serve as focal light scattering [11], in a vessel containing nickel electrolyte by alternating current (AC) or periodic reverse current (PRC) that influences the morphology and composition of electrodeposited nanocrystalline scale of the coatings deposited. [12–15]. The morphology and physical and chemical characteristics of the porous anodic films on aluminium oxide substrates aluminium depend on the type of electrolyte, the concentration, applied voltage, temperature, and anodizing time [16]. The electrolytic nickel impregnation has been studied quite extensively in the

metal salt solutions for electrolytic of anodized aluminium which gives the films optical properties of porous aluminium oxide conversion coating for solar collectors [17-20].

Nickel impregnation of the porous anodic films are produced from a threshold voltage alternating current (5 V AC 50 Hz) and the nickel content in the bottom of the pores increases when the voltage increases, also the negative half cycle is responsible for the action of reduction of  $\text{Ni}^{2+}$ , so the AC voltage plays a very important role during the deposition of nickel in porous anodic films [21].

Our aim was to study the impact of the AC voltage frequency (60 Hz, 180Hz, 360 and 480 Hz) voltage magnitude (10, 11 and 12 Volts), at the times of impregnation constant (2 minutes) and filling fraction of pore volume on the optical properties of the films, specifically in total reflectance, so that these parameters can be correlated with the optical properties coatings.

## 2.- Experimental

Preparation process of selective absorber films requires three consecutive steps: 1) surface pre-treatment 2) anodized aluminium and 3) nickel electrodeposition.

### 2.1) Surface pre-treatment

Aluminium sheet alloy (99.5%) manufactured by Haomei aluminum (Zhengzhou China) were cut into pieces of 22 x 30 x 0.5 mm and hydraulically pressed at 5000 psi, then were annealed in static air at 480°C for 1 hour and slowly cooled to room temperature, were polished mechanically with sandpaper and alumina powders. The samples were degreased and stripped in a solution of sodium carbonate (J.T Baker) 0.25 M at 80°C for three minutes and neutralized in 35% vol. of nitric acid. Finally electropolished at 18 V for 1 minute in a solution of ethanol-per HCl in a ratio 5:1, in every step the samples were washed with deionized water and dried with hot air.

### 2.2).- Anodized aluminium

Anodic oxidation is performed in a solution of 2 M phosphoric acid (J.T. Baker) aluminium samples of 22 x 30 x 0.05 mm. are used as the anode, such as graphite plate counter electrode in an electrochemical cell. There are many variables involved in the anodic oxidation of aluminium, the electrolyte concentration, voltage, temperature, time, etc. In order to optimize the appropriate parameters to the application is performed a detailed investigation of the effects of these variables on the film parameters of porous anodic aluminium oxide (film thickness, barrier layer thickness, pore diameter, distance inter-pore and wall thickness) with constant electrolyte concentration to 2 M (pH=4), the anodization voltage is varied from 10 to 40 V DC and the time of 10 min to 40 min. Anodizing temperature was 18 °C and the distance between electrodes was 2 cm, the current density during the anodization process was 32 mA/cm<sup>2</sup> a 20 V DC at 20 min. After anodizing the samples were washed with deionized water and dried with hot air for 3 min.

### 2.3).- Electrodeposition of Nickel

The electrodeposition of Nickel was carried out in a two-electrode electrochemical cell build with a glass jacket (Dewar vessel) where a nickel plate (99.9%) of 30 x 50 x 1 mm is the counter electrode placed parallel with anodized aluminium plate working electrode. The distance between electrodes was 1.5 cm. and the deposition temperature was 22° C±1. The applied voltages were 10, 11 and 12 V AC and each voltage was used at different frequencies (60 Hz, 180Hz, 360 and 480 Hz). The deposition time was kept constant at 2 minutes. The electrolytic composition for the Nickel deposition was:  $\text{NiSO}_4$  (30 g/l),  $\text{H}_3\text{BO}_3$  (20 g/l)  $(\text{NH}_4)_2\text{SO}_4$  (20 g/l) and  $\text{MgSO}_4$  (20 g/l) and pH = 3.9-4.2 which was previously suggested by J. Salmi [17, 22]. All chemical reagents were of analytical grade (J.T. Baker) and aqueous electrolyte solutions were prepared using deionized water (18  $\Omega/\square$ ).

#### 2.4) Structural and morphology characterization

The images of the samples before and after the impregnation of nickel were acquired by Scanning Electronic Microscopy SEM (SEM) field emission SEM Hitachi S-5500. Compositional-chemical characterization was made by Energy Dispersive Spectroscopy (EDS) use a scanning electron microscope SU1510 Hitachi equipped with detectors for compositional analysis of the samples.

The structure of the porous anodic film impregnated with nickel were analyzed using X-ray Diffraction (XRD) and recorded on a Rigaku D-Max 2200 using Cu-K $\alpha$  radiation ( $\lambda = 0.154056 \text{ \AA}$ ) at angles between  $30^\circ$  and  $90^\circ$ . Diffraction patterns were obtain from Nickel and aluminium substrate, so that the structure of the porous anodic film is considered amorphous with a distribution of nickel particles.

#### 2.5).- Optical characterization

The optical measurement of total reflectance spectra in a range of 250-2500 nm wavelength were measured using a Shimadzu spectrophotometer (Marca y modelo ) equipped with an integration sphere. The reflectance diffuse was measured relative to a BaSO<sub>4</sub> reference. For the measurement of the specular reflectance was measured between 250 and 2500 nm, an evaporated aluminium mirror was used as reference.

### 3.- Results and discussion

The porous anodic films were synthesized at 20V during 20 min, using a solution of 2M H<sub>3</sub>PO<sub>4</sub>, the temperature was controlled by recirculate bath and it was fixed  $18 \pm 2 \text{ }^\circ\text{C}$ . Figure 2 shows the current versus time, which can be divided in four parts (a) correspond to formation of the barrier layer, and during this period the oxide film growth, (b) formation of individual paths in the barrier layer cause for the pore growth, (c) breakdown of individual paths and initiation of pore formation, (d) widening pore and growth of porous oxide layer [25]

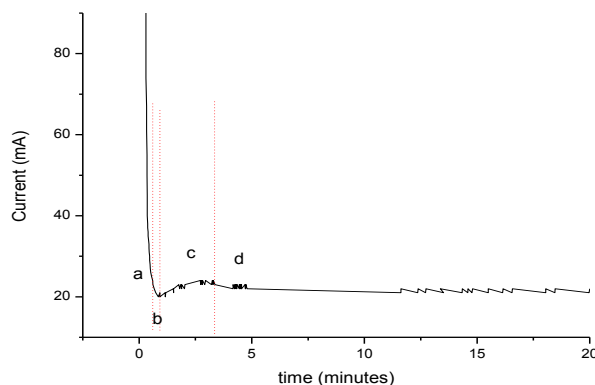


Fig. 2. Current vs. time for the anodized process

The diameter of the pore increase as a function of the applied anodizes potential as it can see in Figure 3. These increments occur for a range potential of 15-30 V and constant time of 20 min. (23). Further studies have reported that the pore diameter depends on the potential or current density according with O'Sullivan [24]. The barrier layer is formed on the basis of the pores and has the same nature as the oxide layer naturally formed on the atmosphere and allows the passage of electric field lines (current). Due to

defects existing only in its structure, the thickness of the barrier layer depends directly of anodizing potential Wernick et al (25) which were corroborated by our experiments. An inspection of Figure 3 indicates that the parameters that are most affected by the anodizing potential are the pore diameter, inter-pore distance, and film thickness on the other hand the wall thickness and the thickness of the barrier layer grown on a small proportion.

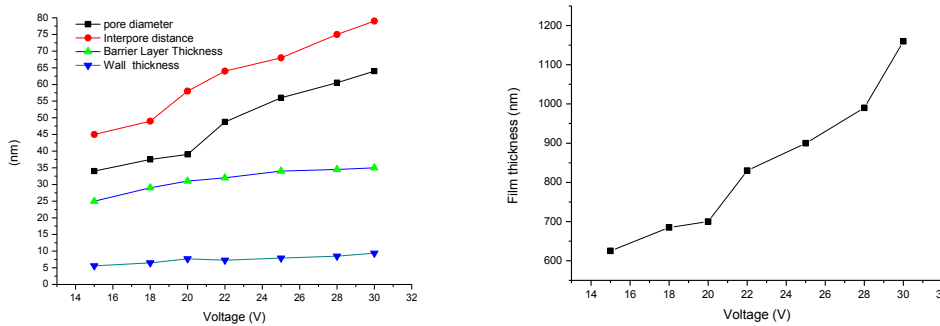


Figure 3 (a) Parameters of porous anodic aluminium films as a function with applied voltage during 20 min. (b) film thickness as a function of applied voltage

Figure 4 shows the Grazing Incidence X-ray Diffraction (GIXD) pattern of Al sample before and after anodized at 30 V CD during 40 min. The main effect of the anodized process was observed in the intensity of the diffraction peaks. Before the anodized process the main diffraction peaks correspond to (220) plane, however after process the previous plane reduce the intensity and increase the (111) plane. This change is probably attributed that during the process the Al atoms in (220) and (200) planes are reduced and the Al atoms in the (111) plane keep almost constant. The highly crystalline is also observed due to the formation of the double diffraction peak at 78.39°.

Table 1 shows the results of atomic composition for the aluminium substrate before and after applied the anodized process (20 volts, 20 min, 2M H<sub>3</sub>PO<sub>4</sub> at 18° C). The main atomic composition before the process is aluminium, in more than 93 at. % that is similar with the reported by the supplier. However, after the anodized process it is observed the increment of oxygen content, it is due to the formation of aluminium oxide in the top substrate. [23].

Table 1 Analysis of the atomic composition of aluminum substrate before and after anodized process at 20V during 20 minutes in a solution of 2 M of H<sub>3</sub>PO<sub>4</sub> at 18°C

Al substrate	Elements (Atomic %)								Total
	O	Mg	Ti	Al	Mn	Ag	P	C	
Before anod. process	6.52	0.1	0.02	93.22	0.1	0.13			100
After anod. process	65.65	-	-	28.71	-	-	0.96	4.68	100

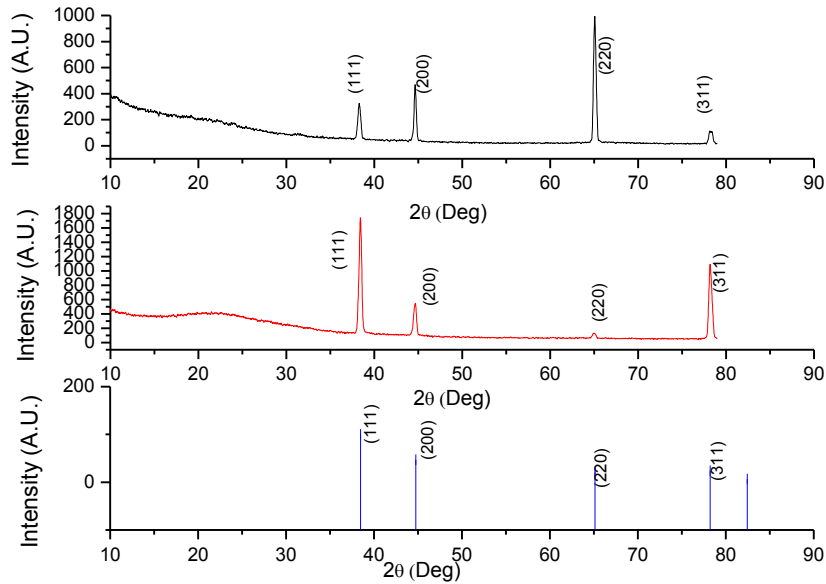


Figure 4. Grazing Incidence X-ray Diffraction (GIXD) pattern of Al 1050 (a) with pre-treatment with sand paper, (b) anodized in 2M phosphoric acid at 30V during 40 min, (c) PDF card # 04-0787 Aluminium

The microphotograph of the anodized aluminium films are show in Figure 5, in Figure 5(a) it can see a top view of the pores build during the anodized process. The average diameter of these pores is 40 nm. A cross section of the alumina layer is in the Figure 5(b) and the estimate thickness is approximately of 700 nm, also from the same figure is possible see the barrier compact layer that has 30 nm of thick, with wall thickness of 8 nm and the inter-pore distance of 60 nm. The compact layer plays an important role in the formation of selective absorber because the right through this layer verifies the heat transfer.

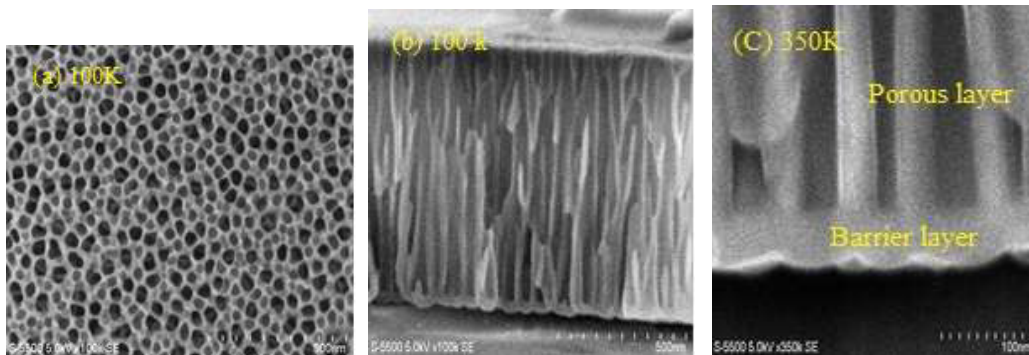


Fig. 5 SEM micrographs of anodized synthesized at 20V /20 min 2M  $H_3PO_4$  at  $18 \pm 2$  °C, (a) surface image to 100K and 30K, (b) cross-section to 100K, (c) cross-section, barrier layer and the bottom of the pores to 350K.

In order to build the selective surfaces with the anodized Al oxide layer it was impregnated with Nickel, using the electrodeposited technique. By use the GIXD technique it can obtained a diffractograph for the sample prepared at 10 V AC with a 60Hz of frequency. Figure 6 shows the X-ray pattern, from this figure it can observer that the (200) and (220) of the Al disappear keeping only the (111) plane, also it is possible to identify the peaks that correspond nickel, in particular (200) and (220) planes. It is an indication that the Nickel was electrodeposited into the oxide aluminium pores.

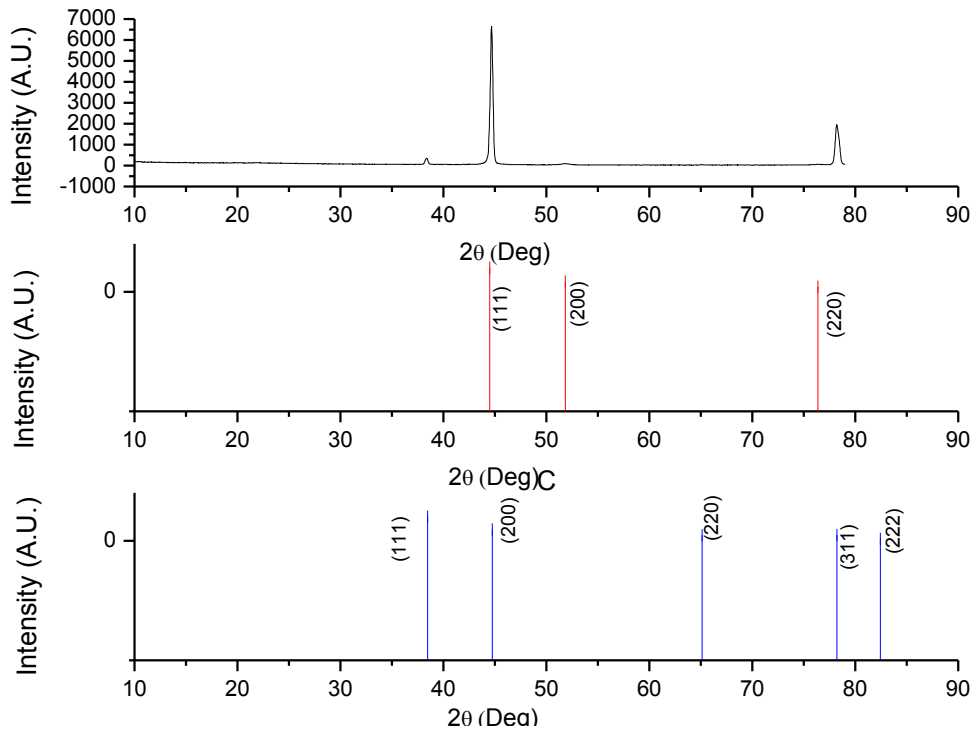


Figure 6. Grazing Incidence X-ray Diffraction (GIXD) pattern of (a)Al<sub>2</sub>O<sub>3</sub>-Ni, (b) JPG Nickel (c) PDF card # 04-0787 Aluminum

Table 2 shows the atomic composition of the aluminum anodized layer impregnated with nickel. The presence of Nickel therein is seen that there is the presence of aluminum (substrate) oxygen, carbon, phosphorus and nickel, shows the presence of Nickel apparently is related to the intensity of the voltage and this process time is as long as a higher voltage and the presence of nickel increases.

Table 2. Analysis of atomic composition of anodic films of aluminium oxide after impregnation with Nickel at 9 V and 10 V de CA (60Hz) during 2 min.

Applied Potential (V)	Atomic composition (%)					Total
	O	Al	C	P	Ni	
9	42.70	50.05	5.75	0.28	1.22	100
10	44.55	44.59	6.38	0.29	3.74	100

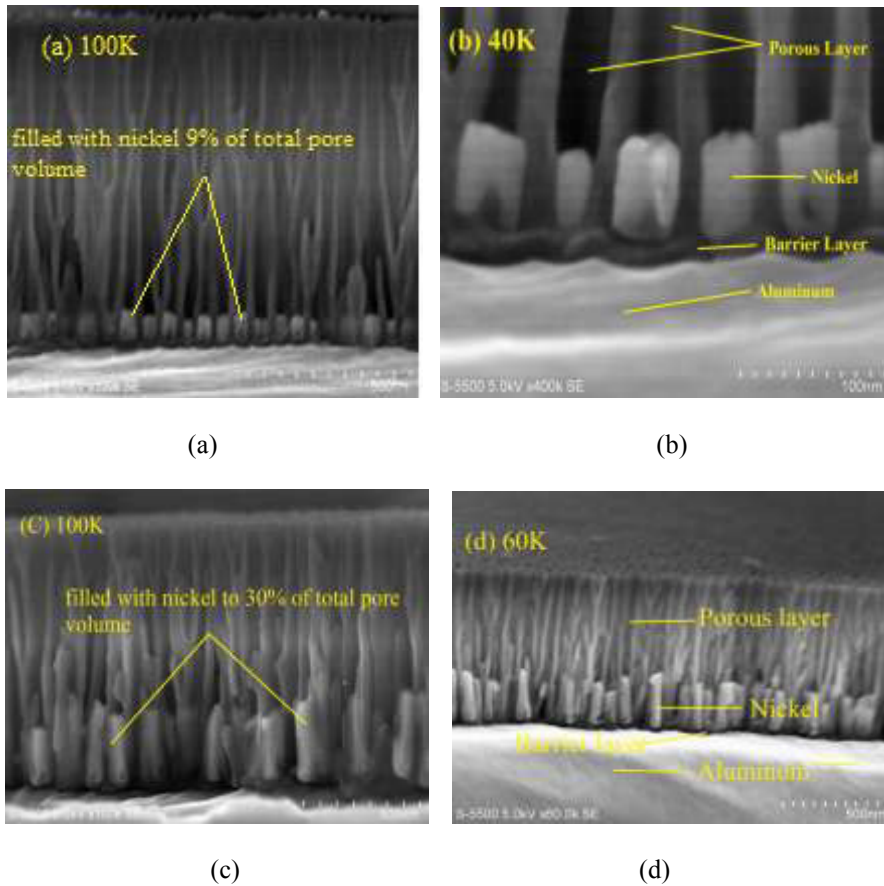


Figure 7 SEM micrographs of cross section of  $\text{Al}_2\text{O}_3$  pores synthesized at 20 V during 20 minutes filled with Ni during 2 minutes at (a) 10 V AC (60 Hz ) and (b) 11V AC (60 Hz)

Figure 7 shows the cross-sections of a porous anodic film with impregnated nickel. The experimental conditions were described above. From this figure it is possible to observe the deposition of nickel into the bottom of the pores. The particles size is smaller than the wavelength of incident radiation. The thickness of nickel into the pore is 69 nm which corresponds to 10% of the total pore volume, however if increase the applied voltage to 11 V AC (60 Hz).

Total reflectance spectra for  $\text{Al}_2\text{O}_3$ -Ni films are shown in Figure 8 (a),(b), and (c). The Nickel deposit films were prepared at three different AC voltages (10, 11 and 12 V), and in every voltage use different frequency (60, 180, 360 and 480 Hz). The deposition time in all cases was 2 min.. Figure 10(a) shows the total reflectance spectrum for  $\text{Al}_2\text{O}_3$ -Nickel films prepared at 10 V. It can observe that the total reflectance into the visible range is almost similar, however  $\lambda_c$  is around 750 nm of wavelength, but when the voltage increase to 11 V,  $\lambda_c$  is close to 1000 nm of wavelength, and if the applied voltage is 12 V this value now is more or less 1250 nm. How, it was describe before [1-3], the spectral selectivity of ideal selective surfaces is define in most of the cases at 1000 nm, for the samples prepared at 11 V are more close to the ideal value. Also, it is important to mention that the frequency has not influence in the



electrodeposition of Nickel, as it can see at low frequency the total reflectance curve is more close to the ideal behavior.

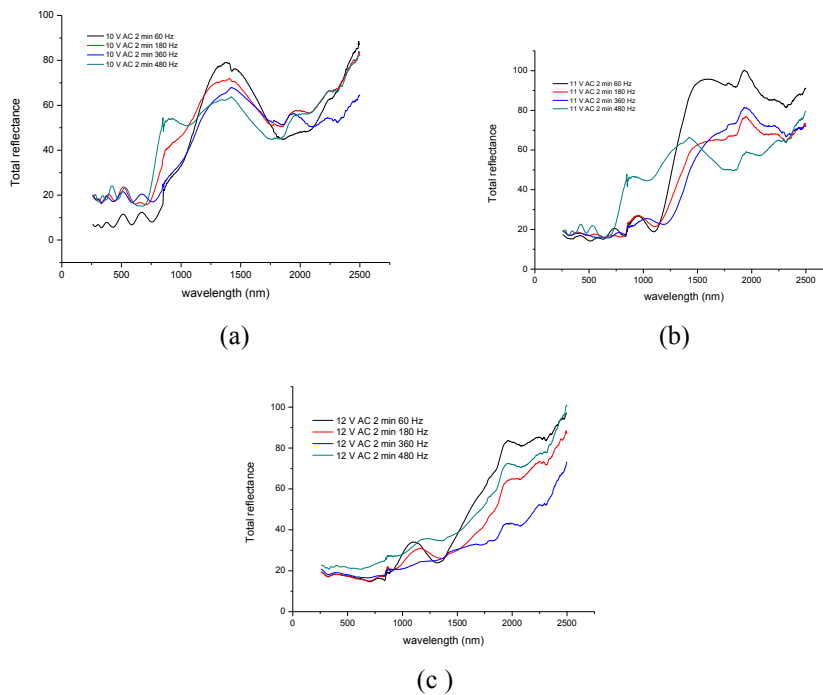


Fig. 8 Spectral reflectance total of  $\text{Al}_2\text{O}_3\text{-Ni}$  (20 V 20 min) at (a) 10 V 2 min at 60, 180, 360 y 48011, (b) 11 V 2 min at 60, 180, 360 y 48011 y 12 V (c) 12 V 2 min at 60, 180, 360 y 480 Hz .

## 5.- Conclusion

This work presented the experimental conditions for growing a selective surface base on oxide aluminum with Nickel. The preparation of the aluminium oxide was made anodic process of Al sheet. By using this process it was formed a layer of aluminium oxide with a thickness of 700 nm and the pore diameter was close to 40 nm. The density of the pores was  $1 \times 10^{10}$  pore/cm<sup>2</sup>. Nickel metal was introduced into the pore using a pulsed electrodeposited technique with AC voltage at different voltage and frequencies. It was found that the influences of high frequencies during the electrodeposition of nickel affect the optical properties, reducing the values of the total reflectivity in the near infrared region, however at low frequencies the cut-off wavelength is close to ideal selective surfaces.

## Acknowledgements

This work was partially supported by CONACYT under the 82306. Also the authors express their gratitude to M.C. Maria Luisa Ramon for XRD measurements and Ing. Rogelio Moran for the SEM analysis and Oscar Gomez-Daza for help in the optical measurements.

## REFERENCES

- [1] H. Tabor, Selective Radiation II. Wavelength Discrimination, *Bull. Res. Council. of Isr. Sect. A: Chem.* 5, 129-134 (1956).
- [2] H. Tabor, Selective Radiation I. Wavelength Discrimination, *Bull. Res. Council. of Isr. Sect. A: Chem.* 5, 119-128 (1956).
- [3] J. T. Gier and R. V. Dunkle, Selective Spectral Characteristics as an Important Factor in the Efficiency of Solar Collectors, *Transaction of the Conference on the Use of Solar Energy* 2, 41- 56 (1955).
- [4] B. O. Seraphin and A. B. Meinel, in: *Optical Properties of Solids-New Developments*, ed. B. O. Seraphin (North-Holland, Amsterdam, 1975) Ch. 17, p. 927.
- [5] D. M. Mattox, *J. Vac. Sci. Technol.* 13 (1976) 127.
- [6] Konate, S., Bes, R. and Traverse, J. P. (1997). *Ann. Chim. Sci. Mat.*, 22, 67.
- [7] Trombe, F., Lephath Vinh, A. and Lephath Vinh, M. (1964). *J. Rech. Cnrs.*, 65, 563.
- [8] Belghith, H.M., Bes, R. S. and Traverse, J. P. (1995). French Patent no. 9508090, 3 juillet.
- [9] Granqvist, C. G., Anderson, A. and Hunderi, O. (1979). *Appl. Phys. Lett.*, 35, 268.
- [10] Granqvist, C. G. (1991). *Materials Science for Solar Energy Conversion Systems*, 1st ed., Chap. 4. Pergamon Press, pp. 74–80.
- [11] Wernick S, Pinner R, Sheasby PG. 5th ed. *The surface treatment and finishing of aluminium and its alloys*, vol. 1 Teddington, Middlesex, UK: Finishing Publications Ltd.; 1996
- [12] Puipe J-C, Leaman F (1986) *Pulse plating*. Eugen G Leuze Verlag, Salgau
- [13] El-Sherik AM, Erb U, Page J (1996) *Surf Coat Technol* 88:70
- [14] Mandich NV (2000) *Met Finish* 98:375
- [15] Landolt D, Marlot A (2003) *Surf Coat Technology* 169–170:8
- [16]. T. Pavlovic and Ignatiev, *Thin Solid Films* 138 (1986) 97.
- [17] Keller, F., Hunter, MS and Robinson, D. L. (1953) *J. Electrochem. Soc.*, 100, 411-419.
- [18] Salmi J, Bonino J-P, Bes RS (2000) *J Mater Sci* 35:1347
- [19] Shaffei MF, Abd El-Rehim SS, Shaaban NA, Huisen HS (2001) *Renew Energy* 23:489
- [20] Bostrom T, Wäckelgard E, Westin G (2003) *Sol Energy* 74:497
- [21] Arurault L, Salmi J, Bes RS (2004) *Sol Energy Mater Sol Cells* 82:447
- [22] Salmi J, Bes RS (2004) *Sol Energy Mater Sol Cells* 82:447
- [23] Doughty AS, Thompson GE, Richardson JA, Wood GC. Investigation of the electrolytic colouring of porous anodic films on aluminium using electron microscopy. *Trans Inst Met Finish* 1975;53:33.
- [24] Dionisio R. Electrolytic coloring process. US Patent 4, 421, 610 (1983)
- [25] Zhao Y, Chen M, Zhang Y, Xu and Liu W T: *Mater Vol Lett* 405 (2005), p. 456
- (26) O'Sullivan, J.P. and Wood, G.C. (1970) *Proc. Roy. Soc. Lond. A*, 317, 511–543
- [27] Wernick, S., Pinner, R. and Sheasby, P.G. (1987) in *The Surface Treatment and Finishing of Aluminum and its Alloys*, ASM International, Finishing Publication Ltd., 5th edition, pp. 289–368.
- [28] C.K. Preston, M. Moskovits, *J. Phys. Chem.* 97 (1993) 8495–8503.